Inorganic Chemistry

Article

pubs.acs.org/IC

Hydrogen Bonding and Electron Transfer between Dimetal Paddlewheel Compounds Containing Pendant 2-Pyridone Functional Groups

Luke A. Wilkinson, Laura McNeill, Paul A. Scattergood, and Nathan J. Patmore*

Department of Chemistry, University of Sheffield, Sheffield S3 7HF, U.K.

Supporting Information

ABSTRACT: The compounds $M_2(TiPB)_3(HDON)$ (TiPB = 2,4,6-triisopropylbenzoic acid; H_2DON = 2,7-dihdroxy-1,8-napthyridine; M = Mo (**1a**) or W (**1b**)) and $Mo_2(TiPB)_2(O_2CCH_2Cl)(HDON)$ (**1c**) which contain a pendant 2-pyridone functional group have been prepared. These compounds are capable of forming self-complementary hydrogen bonds, resulting in the formation of "dimers of dimers" ($[\mathbf{1a-c}]_2$) in CH_2Cl_2 solutions. Electrochemical studies reveal two successive one-electron redox processes for $[\mathbf{1a-c}]_2$ in CH_2Cl_2 solutions that correspond to successive oxidations of the dimetal core, indicating stabilization of the mixed-valence state. Only small changes in the value of K_c are observed upon changing the ancillary ligand or metal, implying that proton coupled mixed valency is responsible for the stabilization. Dimethylsulfoxide (DMSO) disrupts the hydrogen bonding interactions in these compounds, and a single oxidation process is observed in DMSO which shifts to lower potential as the number of HDON ligands increases. Further substitution of carboxylate ligands with HDON leads to the formation of $Mo_2(TiPB)_2(HDON)_2$ (**2**) and $Mo_2(HDON)_4$ (**3**), which adopt *trans*-1,1 and *cis*-2,2 regioisomers in the solid-state. ^{1}H NMR spectroscopy indicates that there are at least two regioisomers present in solution for both compounds. The lowest energy transition in the electronic absorption spectra of these compounds corresponds to a M_2-$\delta \rightarrow$ HDON-π^* transition. The electrochemical, spectroscopic and structural results were rationalized with the aid of density functional theory (DFT) calculations.

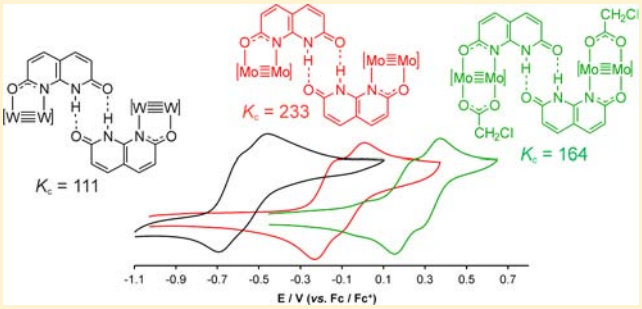

INTRODUCTION

Dimetal paddlewheel compounds have four ligands bridging the dimetal core in the equatorial sites and two axial sites which are available for coordination by donor ligands or solvent.[1] The well-defined coordination environment makes them good candidates as building blocks for the synthesis of metal−organic frameworks,[2] having potential applications in areas such as gas sorption,[3] catalysis,[4−7] magnetic materials,[8−10] or as building blocks in coordination polymers for use in molecular electronic devices.[11−16] These materials typically employ rigid organic bridging ligands that rely on metal−ligand interactions to propagate one-, two-, or three-dimensional architectures.

Metal−metal quadruply bonded paddle compounds are redox active, with the dimetal core readily losing one or more electrons.[17−19] The redox potential can be tuned by changing the nature of the bridging ligand,[20] and recent studies from Berry and co-workers have also demonstrated, using a series of M≡M···M′ compounds, that axially coordinated metal ions can be used to influence the redox behavior of the quadruple bond.[21−23] Quadruply bonded dimetal compounds also have interesting photophysical properties.[24,25] For example, the compounds $M_2(TiPB)_4$ (M = Mo, W; TiPB = 2,4,6-triisopropylbenzoate) show emission from a long-lived (Mo, τ = 43 μs; W, τ = 1.6 μs) metal-based T_1 state, the $^3M_2\delta\delta^*$.[26] Recent investigations by Chisholm and co-workers have also used transient absorption and time-resolved infrared spectroscopy to elucidate the nature of the singlet and triplet states in a family of mixed ligand compounds of form *trans*-$M_2(TiPB)_2(L)_2$ (M = Mo, W; L = conjugated carboxylate or amidinate bridging ligand).[25,27,28] Interestingly, studies on these compounds have revealed that in the metal-to-ligand charge-transfer (MLCT) states, the single electron on the ligands (L) is fully delocalized over both ligands.[29,30] Delocalization is a result of strong $M_2\delta$-Lπ conjugation, a property which has been employed extensively to study ground state electron transfer in "dimers of dimers", which consist of two dimetal units bridged by a conjugated ligand.

The redox, photophysical, and electron transport properties of MM quadruple bonds have made them attractive targets for incorporation into functional materials.[31−34] Dicarboxylate bridges are often employed as linkers to generate molecular triangles,[35,36] and squares.[37,38] Recent work by Zhou and co-workers has also demonstrated that the shape and size of molecular architectures incorporating quadruple bonds can be

Received: June 19, 2013
Published: August 8, 2013

   dx.doi.org/10.1021/ic401555g | *Inorg. Chem.* 2013, 52, 9683−9691

controlled by varying the bridging angle and size of the dicarboxylate linker.[39]

There is significant interest in developing metal complexes containing pendant hydrogen bond donor−acceptor groups, as the hydrogen bond is directional and can self-assemble to form a variety of architectures.[40−42] However, there have been relatively few examples of using hydrogen bonding as a tool to generate self-assembled architectures containing dimetal paddlewheel building blocks.[43,44] We have recently reported the synthesis of $Mo_2(TiPB)_3(HDON)$ (H_2DON = 2,7-dihydroxy-1,8-naphthyridine) and $Mo_2(TiPB)_3(HDOP)$ (H_2DOP = 3,6-dihydroxypyridazine) which form hydrogen bonded "dimers of dimers" in CH_2Cl_2.[45] Electrochemical studies demonstrated that the mixed-valence states of these dimers are stabilized upon oxidation by one-electron. The absence of an intervalence-charge transfer band in the NIR region of their electronic absorption spectra indicate that these are rare examples of proton-coupled mixed valency, in which electron transfer is dependent on the proton coordinate.[46]

In this investigation we report the synthesis of a family of compounds of form $Mo_2(TiPB)_{4-n}(HDON)_n$ (n = 1, 2, or 4), which contain a pendant 2-pyridone functional group that can act as hydrogen bond donor−acceptor, and are novel building blocks for hydrogen bonded assemblies. Changes in the energy of the M_2-δ orbitals which act as the donor and acceptor have a dramatic impact on the extent of electronic coupling in covalently bound M_2-bridge-M_2^+ systems, and provide valuable insight into possible superexchange mechanisms.[47] Therefore we will also investigate the effect that changing the metal (M = Mo or W) or ancillary ligand (O_2CR) has on the stability of mixed valence hydrogen-bonded "dimers of dimers".

RESULTS AND DISCUSSION

Synthesis. The series of dimetal paddlewheel compounds containing pendant 2-pyridone functional groups used in this study were synthesized by reaction of $M_2(TiPB)_4$ (M = Mo, W; TiPB = 2,4,6-triisopropylbenzoate; Scheme 1) or $Mo_2(O_2CCH_3)_4$ with H_2DON (2,7-dihydroxy-1,8-naphthyridine; Scheme 1). The number of pendant hydrogen bond donor−acceptor ligands was controlled by the reagent stoichiometry and reaction conditions; elevated temperatures are needed to append four H_2DON ligands. Compounds with one, $M_2(TiPB)_3(HDON)$ (M = Mo, **1a**; M = W, **1b**), two, $Mo_2(TiPB)_2(HDON)_2$ (**2**), and four, $Mo_2(HDON)_4$ (**3**), appended HDON ligands were synthesized. Reaction of **1a** with 1 equiv of chloroacetic acid generated $Mo_2(TiPB)_2(O_2CCH_2Cl)(HDON)$, **1c**, and drawings of all the ligands and compounds used in this study are shown in Scheme 1.

Scheme 1. Ligands and Compounds Employed in This Study

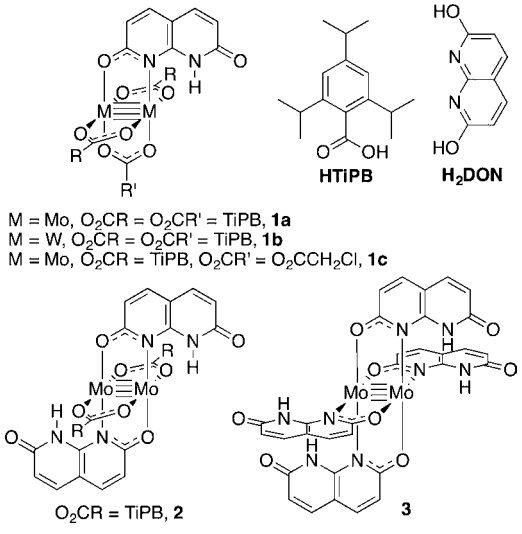

Ditopic ligands such as H_2DON are capable of coordinating two dimetal units to form "dimers of dimers" or other oligomers. The use of the bulky TiPB ancillary ligands was essential in this study as it prevents ligand scrambling or coordination of another dimetal unit to form mixtures of unwanted oligomeric species.[48] Compounds [**1a−c**] are soluble in most organic solvents, whereas compound **2** is soluble in donor solvents such as tetrahydrofuran (THF), and compound **3** is only sparingly soluble in strong donor solvents such as dimethylsulfoxide (DMSO). Matrix-assisted laser desorption/ionization time-of-flight (MALDI-TOF) mass spectrometry of all compounds showed the expected molecular ions corresponding to the products.

X-ray Crystallography. Despite extensive efforts, we have been unable to isolate crystals of **1a−c** suitable for X-ray diffraction from coordinating or noncoordinating solvents. We were however able to obtain crystals of $2(DMSO)_2{\cdot}4DMSO$ and $3(DMSO)_2{\cdot}2DMSO$ from DMSO solutions. The crystal structures of these compounds are shown in Figures 1 and 2, with selected bond lengths and angles in Table 1.

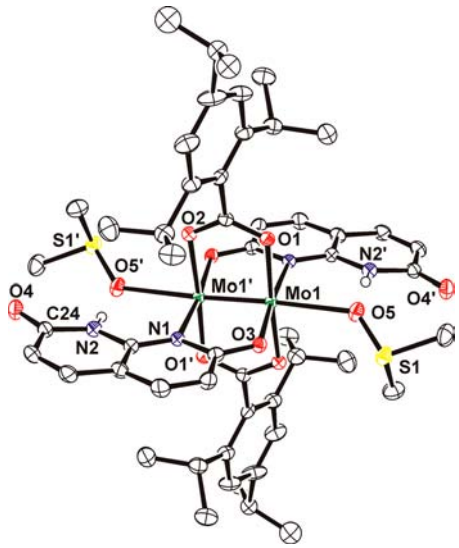

Figure 1. Molecular structure of $2(DMSO)_2$ with anisotropic displacement parameters drawn at the 40% level and all hydrogen atoms (except those associated with the lactam functional groups) omitted for clarity. The molecule sits on an inversion center, and atoms with an additional prime (′) character are generated from the corresponding atoms without the prime label by an inversion operation.

Both compounds sit on a crystallographic inversion center and have the expected paddlewheel arrangement of the ligands about the dimetal core. The Mo1−Mo1′ bond lengths of 2.1042(6) Å (**2**$(DMSO)_2$) and 2.1026(15) Å (**3**$(DMSO)_2$) are consistent with a formal metal−metal quadruple bond.[1] The Mo−O bond lengths of the axially coordinated DMSO molecules are similar to those found in other

dx.doi.org/10.1021/ic401555g | Inorg. Chem. 2013, 52, 9683−9691

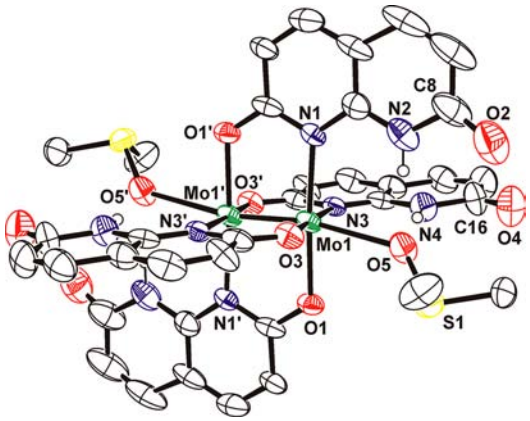

Figure 2. Molecular structure of $3(DMSO)_2$ with anisotropic displacement parameters drawn at the 40% level and all hydrogen atoms (except those associated with the lactam functional groups) omitted for clarity. The molecule sits on an inversion center, and atoms with an additional prime (′) character are generated from the corresponding atoms without the prime label by an inversion operation.

$Mo_2(O_2CR)_4(DMSO)_2$ compounds.[49] The DMSO molecules also form hydrogen bonds with the N−H protons of the HDON ligand. The C═O bond lengths in the free amide functional groups of the HDON ligand are relatively short for $2(DMSO)_2$ and $3(DMSO)_2$ (<1.26 Å). This is consistent with the compounds adopting the lactam tautomer in the solid-state.[50]

As well as potential tautomeric isomers, paddlewheel compounds containing bridging ligands with inequivalent binding atoms can adopt a number of different regioisomers, as shown in Scheme 2.[20,51−53] The solid state structure of $2(DMSO)_2$ shows that the ligands adopt a *trans*-1,1 isomeric form in the solid state, whereas for $3(DMSO)_2$ the ligands adopt a *cis*-2,2 arrangement.

Solution Behavior. The structure of 2-pyridone in the gas-phase, solution, and solid-state has been extensively studied as it is a good model for understanding hydrogen bonding in DNA base pairs.[54,55] It undergoes lactim/lactam tautomerism and can dimerize to form a number of cyclic dimers. We have previously shown using diffusion-ordered ^1H NMR spectroscopy that $Mo_2(TiPB)_3(HDOP)$ (H_2DOP = 3,6-dihydroxypyridazine) forms the hydrogen bonded "dimer of dimers" $[Mo_2(TiPB)_3(HDOP)]_2$ in CD_2Cl_2 solutions, but addition of

Scheme 2. Different Possible Regioisomers for 2 and 3

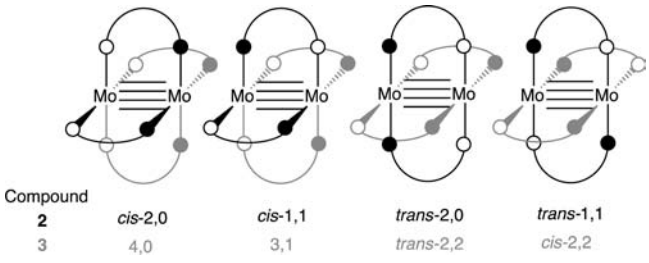

DMSO disrupts the hydrogen bonding to form a monomer.[45] The same behavior was observed for $[\mathbf{1a}]_2$, and the ^1H NMR spectra of $[\mathbf{1a}]_2$ in CD_2Cl_2 at 5.0, 2.5, and 0.5 mM concentrations are shown in the Supporting Information. No new peaks are observed upon dilution, and there is no change in the chemical shift or broadening observed for the NH proton at δ 12.29. In addition, there are no changes observed in the ^1H NMR spectrum upon cooling to 203 K. This indicates that the association constant for the monomer−dimer equilibrium (Scheme 3) must be relatively high, and that there will only

Scheme 3

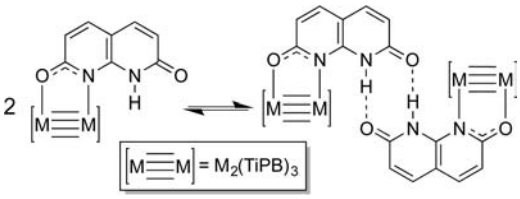

be minor concentration effects in the concentration range used for spectroscopic and electrochemical measurements. In addition, the single peak indicates that the dimer adopts the lactam−lactam tautomer exclusively in solution.

DMSO is known to disrupt hydrogen bonding, and in DMSO or CH_2Cl_2/DMSO solvent mixtures the monomer **1a** is generated. The ^1H NMR spectra of $[\mathbf{1a}]_2$ in CD_2Cl_2 and **1a** in a CD_2Cl_2/DMSO-d_6 (4:1) mixture are compared in Figure 3. The NH proton resonance shifts to δ 10.30 for **1a**, and there is no shift of this peak or evidence of a lactim tautomer forming for **1a** in CD_2Cl_2/DMSO-d_6 (4:1) solution at low temperature (203 K).

The IR spectra of $[\mathbf{1a}]_2$ and **1a** were recorded in CH_2Cl_2 and CH_2Cl_2/DMSO (20:1) solutions respectively, and are shown in

Table 1. Selected Bond Lengths (Å), Angles (deg), and Torsion Angles (deg) for $2(DMSO)_2$ and $3(DMSO)_2$

$2(DMSO)_2$		$3(DMSO)_2$	
Mo1−Mo1′	2.1042(6)	Mo1−Mo1′	2.1026(15)
Mo1−O1	2.122(3)	Mo1−O1	2.095(5)
Mo1′−O2	2.117(3)	Mo1−O3	2.084(5)
Mo1−O3	2.088(3)	Mo1−N1	2.184(7)
Mo1′−N1	2.204(3)	Mo1−N3	2.203(6)
Mo1−O5	2.542(3)	Mo1−O5	2.535(6)
C24−O4	1.243(5)	C8−O2	1.255(13)
N2···O5′	2.809(5)	C16−O4	1.235(11)
Mo1′−Mo1−O5	170.91(7)	N2···O5	2.775(10)
O1−Mo1−Mo1′−O2	0.91(11)	N4···O5	2.778(9)
O3−Mo1−Mo1′−N1	2.47(12)	Mo1′−Mo1−O5	168.54(14)
		N1−Mo1−Mo1′−O1′	1.9(2)
		O3−Mo1−Mo1′−N3′	1.2(2)

dx.doi.org/10.1021/ic401555g | *Inorg. Chem.* 2013, 52, 9683−9691

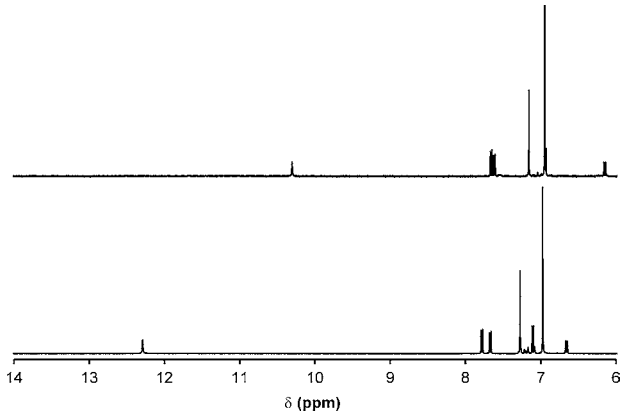

Figure 3. Low-field region of the ^{1}H NMR spectra of $[\mathbf{1a}]_2$ (2.5 mM in CD_2Cl_2; bottom) and **1a** (5.0 mM in DMSO-d_6/CD_2Cl_2 (4:1) mixture; top).

the Supporting Information. A weak band appears at 2800 cm^{-1} for $[\mathbf{1a}]_2$, which could be assigned to the NH stretch of the HDON ligand, and for **1a** a weak broad band appears around 3040 cm^{-1}. The ν(C═O) stretch of the lactam tautomer for $[\mathbf{1a}]_2$ and **1a** appears at 1644 and 1672 cm^{-1}, respectively. Once again there is no obvious evidence of tautomerism in solution in agreement with the ^{1}H NMR spectroscopy data.

The ^{1}H NMR spectrum for **2** in DMSO-d_6 indicates that there are two species in solution. Two resonances are observed at δ 10.23 and 10.16 in the low-field region of **2** in the ratio 1.7: 1, and two sets of HDON and aromatic TiPB resonances can also be distinguished in the same ratios. Based on the solution behavior of **1a**, and the similar chemical shift of the low-field resonances, these peaks are likely to correspond to different regioisomers (see Scheme 2) rather than tautomers. The most abundant species is assigned to the *trans-1,1* regioisomer, as observed in the solid-state. Based on the density functional theory (DFT) calculations, vide infra, we tentatively assign the less abundant regioisomer as the *trans-2,0*.

Evidence of regioisomerism is also seen in the ^{1}H NMR spectrum of **3**. Three resonances are observed at δ = 10.28, 10.16, and 9.94 in a ratio of 1.0: 1.3: 1.7. Again, we assume that these resonances correspond to the presence of at least two different regioisomers for **3** in solution, although only one regioisomer was observed in the solid-state.

Electrochemistry. The cyclic voltammogram of compound $[\mathbf{1a}]_2$ in CH_2Cl_2 has been previously reported,[45] and shows two successive one-electron redox processes separated by 140 mV. The successive one-electron oxidations indicate that the mixed valence state is stabilized with respect to its neutral and doubly oxidized forms. The comproportionation constant (K_c; Scheme 4)[56] for $[\mathbf{1a}]_2$ is 233.

The magnitude of K_c is often correlated to the extent of electronic coupling in mixed valence compounds, and large values (>10^6) are often indicative of Class III (fully delocalized) behavior in mixed valence compounds of form M-B-M$^+$. Although K_c is a useful guide to the extent of stabilization of the mixed valence state when comparing similar systems, several groups have pointed out that care needs to be taken when comparing values in different systems as it is an equilibrium constant which can be affected by a variety of factors.[57,58] However, conclusions can be drawn about trends in the magnitude of K_c in similar systems employing the same electrolyte. For M_2-B-M_2^+ compounds, strong coupling is observed with relatively modest K_c values by comparison to M-B-M$^+$ systems, as any charge is more diffuse in dimetal compounds.[59]

Scheme 4

$$[\mathbf{1a}]_2 + [\mathbf{1a}]_2^{2+} \underset{}{\overset{K_c}{\rightleftharpoons}} 2[\mathbf{1a}]^+$$

$$K_c = e^{(\Delta E_{1/2}/25.69)} \text{ (at 298 K)}$$

The voltammograms for $[\mathbf{1a}]_2$, $[\mathbf{1b}]_2$, and $[\mathbf{1c}]_2$ are shown in Figure 4, and the data are summarized in Table 2. All of the

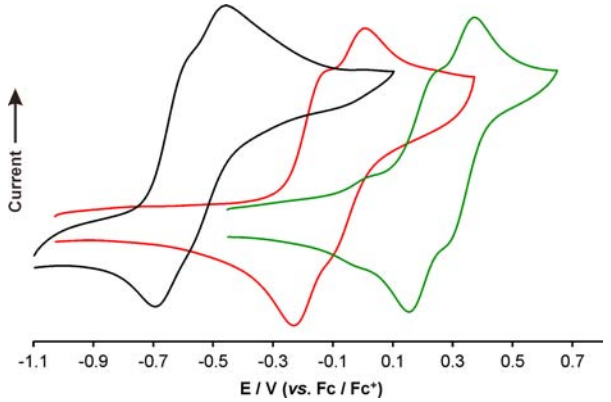

Figure 4. Cyclic voltammograms of $[\mathbf{1a}]_2$ (red), $[\mathbf{1b}]_2$ (black), and $[\mathbf{1c}]_2$ (green) in 0.1 M NBu_4PF_6/CH_2Cl_2 solutions.

Table 2. Electrochemical and Spectroscopic Data for All Compounds

compound	solvent	$E_{1/2}(1)$/V[a]	$E_{1/2}(2)$/V[a]	$\Delta E_{1/2}$/mV	K_c[b]	M_2-δ → HDON-π^* λ_{max}/nm[c]
$[\mathbf{1a}]_2$	CH_2Cl_2	−0.182	−0.042	140	233	
1a	CH_2Cl_2/DMSO[d]	−0.131				430
$[\mathbf{1b}]_2$	CH_2Cl_2	−0.637	−0.516	121	111	
1b	CH_2Cl_2/DMSO[d]	*−0.716*[e]				573
$[\mathbf{1c}]_2$	CH_2Cl_2	0.199	0.330	131	164	
1c	CH_2Cl_2/DMSO[d]	−0.026				421
2	CH_2Cl_2/DMSO[d]	−0.131				448
3	DMSO	−0.250				461

[a]Potential vs Fc/Fc$^+$. [b]Obtained from the equation K_c = e($\Delta E_{1/2}$/25.69). [c]All spectra obtained in DMSO solutions at room temperature. [d]Obtained by addition of 100 μL of DMSO to an electrochemical cell containing 4 mL of a 0.1 M NBu_4PF_6/CH_2Cl_2 solution. [e]Irreversible.

dimers show two redox processes corresponding to successive oxidations of the Mo_2^{4+} dimetal cores. Previous studies on $[\mathbf{1a}]_2$ indicated that stabilization of the mixed-valence state is likely to be due to proton-coupled mixed valency, in which electron transfer between the dimetal units is dependent on the proton coordinates of the hydrogen bonds, as opposed to electronic coupling via a superexchange mechanism involving direct overlap of the donor, bridge, and acceptor orbitals.[45] Comparison of the K_c values for $[\mathbf{1a}]_2$ (K_c = 233) and $[\mathbf{1b}]_2$ (K_c = 111) support this assignment. The K_c values for Mo_2-B-Mo_2^+ and W_2-B-W_2^+ systems with covalent bridges differ by

dx.doi.org/10.1021/ic401555g | Inorg. Chem. 2013, 52, 9683−9691

many orders of magnitude as the W_2-δ orbitals are ~0.5 eV higher in energy than for molybdenum, and they overlap more effectively with the bridge π-orbitals.[47,60] For example, for $[M_2(O_2C^tBu)_3](\mu$-2,5-dihydroxyterephthalate$)^+$ K_c is 21 for M = Mo, but increases to 2600 for M = W.[61] Therefore, while there is an effect on changing Mo ($[\mathbf{1a}]_2$) to W ($[\mathbf{1b}]_2$), the magnitude of change in K_c is not consistent with electronic coupling being the primary mechanism by which the mixed valence state is stabilized.

The addition of the electron withdrawing chloroacetate group in $[\mathbf{1c}]_2$ results in a small reduction in K_c by comparison to $[\mathbf{1a}]_2$. While the change of metal and ancillary ligand has a significant effect on the redox potential of the dimetal core, it will not significantly affect the properties of the bridging ligands, and hence only a small effect is seen on the value of K_c. Proton-coupled electron transfer can occur via sequential electron (ET) and proton (PT) transfer, or stepwise mechanisms (ET-PT or PT-ET), and elucidating a mechanism is often complicated.[62,63] The subtle effect that metal or ancillary ligand changes have on the extent of stabilization of the mixed valence states of $[\mathbf{1a-c}]_2$ makes it difficult to draw any conclusions about possible mechanisms for proton-coupled mixed valency in these systems. However, we anticipate that addition of electron-donating and -withdrawing substituents to the bridging ligands will have a more substantial impact and permit proposal of a possible mechanism in future work.

Addition of a small amount of DMSO to the electrochemical cell containing compounds $[\mathbf{1a-c}]_2$ results in the formation of the monomers **1a–c**, as evidenced in their cyclic voltammograms (Figure S3, Supporting Information) which now display a single oxidation process. As anticipated, the electron withdrawing chloroacetate group makes **1c** the most difficult compound to oxidize, whereas the tungsten compound **1b** has the lowest oxidation potential.

The cyclic voltammograms of **1a**, **2**, and **3** are compared in Figure 5. Despite evidence for the presence of different

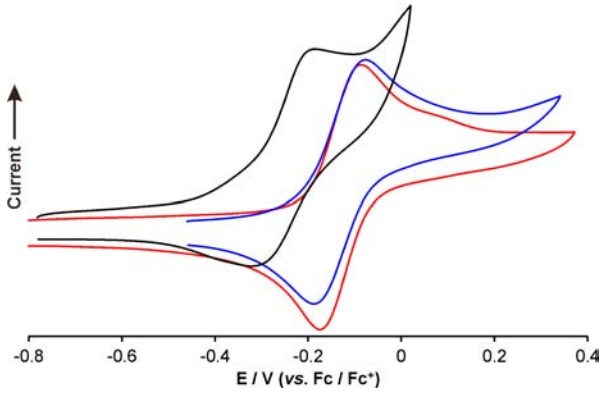

Figure 5. Cyclic voltammograms of **1a** (red), **2** (blue), and **3** (black) in 0.1 M NBu_4PF_6 solutions of CH_2Cl_2/DMSO (**1a**) or DMSO (**2** and **3**).

regioisomers in the ^{1}H NMR spectra of **2** and **3**, only a single oxidation is observed for these species indicating that the regioisomers have similar electronic properties. The HDON ligand is likely to be a better π-acceptor ligand than HTiPB, in which case the oxidation potential of the Mo–Mo quadruple bond is expected to increase as 1, 2, and 4 HDON ligands are added to the dimetal core. In fact, the Mo_2^{4+}/Mo_2^{5+} potentials of all compounds are very similar, and it actually decreases by a small amount for **3**, which has 4 HDON ligands. This implies that as well as acting as a π-acceptor, the HDON ligand is also acting as π-donor.

UV/vis Spectroscopy. The UV/vis spectra of all compounds in DMSO are shown in Figure 6, with data

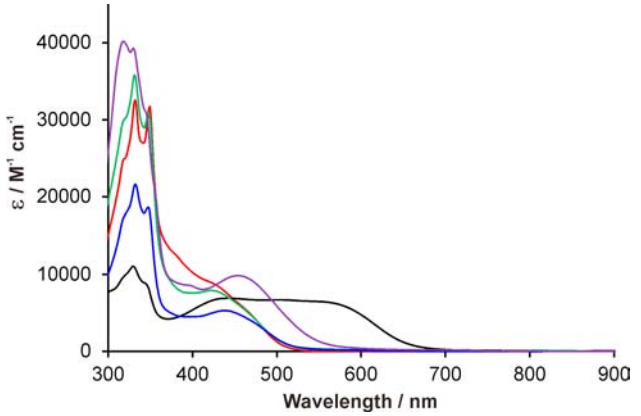

Figure 6. UV/vis spectra of **1a** (red), **1b** (black), **1c** (green), **2** (blue), and **3** (purple) recorded in DMSO at room temperature.

provided in Table 2. All Mo_2 compounds display intense absorptions around 330 nm which result from a combination of the Mo_2-$\delta \rightarrow$ TiPB-π^* and HDON-$\pi \rightarrow$ HDON-π^* transitions. For **1b**, the W_2-$\delta \rightarrow$ TiPB-π^* MLCT transition is shifted to lower energy because of the increase in energy of the W_2-δ orbital by comparison to molybdenum. Two additional transitions are observed at 446 and 510 nm which are due to the two different TiPB environments in the molecule.

The lowest energy transition in each instance is assigned as the M_2-$\delta \rightarrow$ HDON-π^* MLCT transition. This transition slightly decreases in energy as the number of HDON ligands in the complex increases.

Theoretical Studies. To help rationalize the solution behavior of these compounds, DFT calculations have been performed using Gaussian09 at the M06/SDD and 6-311G(d,p) level of theory using the model compounds $Mo_2(O_2CH)_3$(HDON) (**1a′**), $W_2(O_2CH)_3$(HDON) (**1b′**), *trans-1,1*-$Mo_2(O_2CH)_2(HDON)_2$ (**2′**), and *cis-2,2*-$Mo_2(O_2CH)_2(HDON)_2$ (**3′**). Formate groups have been used in place of TiPB to reduce computational time.

The relative stabilities of the three other regioisomers for **2′** were calculated, and found to be just 0.8 (*trans-2,0*), 1.9 (*cis-1,1*), and 2.2 (*cis-2,0*) kJ mol^{-1} less stable than the *trans-1,1* regioisomer. This is consistent with the ^{1}H NMR data for **2** which indicated the presence of two regioisomers in solution, tentatively assigned as the *trans-1,1*, and *trans-2,0* regioisomers based upon the solid-state structure and these calculations. The spectroscopic and electrochemical data indicate that regioisomerism does not significantly influence the electronic structure of the dimetal core, so subsequent discussion will focus on the *trans-1,1* and *cis-2,2* regioisomers of **2′** and **3′** observed in the solid-state.

The geometries for all compounds were optimized using a PCM solvation model in DMSO without symmetry constraints; for each compound the lactam tautomer was calculated to be the most stable form. Calculated bond lengths are given in Table 3. The calculated Mo–Mo and W–W bond lengths (~2.10 and 2.20 Å) are consistent with those found for quadruply bonded $M_2(O_2CR)_4$ compounds,[1] and there is

dx.doi.org/10.1021/ic401555g | Inorg. Chem. 2013, 52, 9683–9691

Table 3. Calculated Bond Lengths (Å) for 1a′, 1b′, 2′, and 3′[a]

	1a′ (M = Mo)	1b′ (M = W)	2′ (M = Mo)	3′ (M = Mo)
M−M	2.109	2.203	2.103 (2.1042(6))	2.095 (2.1026(15))
$M-N_{(HDOP)}$	2.211	2.191	2.222 (2.204(3))	2.238[a] (2.194(9))[a]
$M-O_{(HDOP)}$	2.089	2.080	2.097 (2.088(3))	2.098[a] (2.090(7))[a]
$M-O_{(cis\text{-}TiPB)}$	2.143[a]	2.140	2.148[a] (2.120(4))[a]	
$M-O_{(trans\text{-}TiPB)}$	2.148[a]	2.140		
$C{=}O_{(HDON)}$	1.220	1.220	1.220 (1.243(5))	1.220[a] (1.245(17))[a]

[a]Experimentally observed values for $2(DMSO)_2$ and $3(DMSO)_2$ have been included in parentheses.

excellent agreement between the calculated and observed bond lengths for 2′ and 3′

The frontier MO energy level diagrams calculated for 1a′, 1b′, 2′, and 3′ are shown in Figure 7, and selected frontier

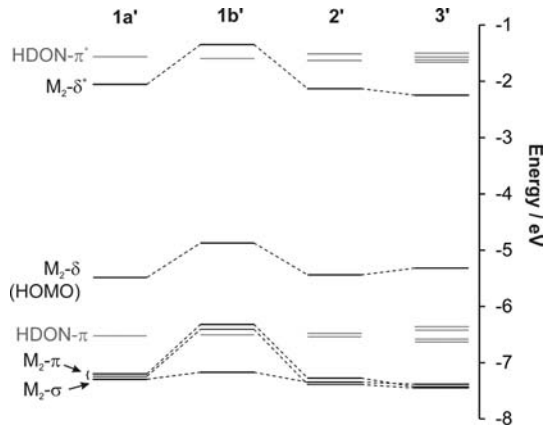

Figure 7. Calculated frontier MO energy level diagrams for 1a′, 1b′, 2′, and 3′.

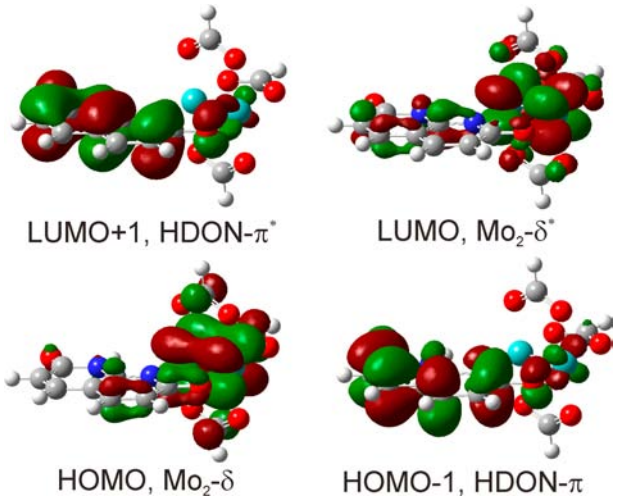

Figure 8. Gaussview plots of selected orbitals for 1a′.

molecular orbital diagrams for 1a′ are shown in Figure 8. The HOMO in each instance is the M_2-δ, and the LUMO is the M_2-δ* when M = Mo and HDON-π* when M = W. The proximity of both the HDON-π and -π* orbitals to the M_2-δ orbitals means the HDON ligand could potentially act as either a π-donor or π-acceptor ligand, and the compound with four HDON ligands (3′) has the highest HOMO energy of all the dimolybdenum compounds. The calculations are consistent with the electrochemical data, in which 3 has a lower oxidation potential than 1a and 2.

CONCLUSIONS

A series of compounds with 1, 2, or 4 HDON ligands has been synthesized. The pendant 2-pyridone functional groups can form self-complementary double hydrogen bond interactions, and compounds 1a−c dimerize in CH_2Cl_2 solutions. Cyclic voltammetry shows stabilization of the mixed valence state in these compounds, and the modest effect observed on the values of K_c by changing the metal or ancillary ligands is consistent with proton-coupled mixed valency being responsible for the electron self-exchange, as opposed to a mechanism involving overlap of donor, bridge, and acceptor orbitals.

These compounds are rare models for the study of electron transfer processes through hydrogen-bond assemblies relevant to biological processes, such as interstrand proton-coupled electron transfer in DNA. In addition, the controlled substitution chemistry and well-defined coordination geometry about the dimetal core makes these compounds potential building blocks for the development of functional hydrogen bonded assemblies.

EXPERIMENTAL SECTION

Physical Methods. MALDI-TOF spectrometry data was collected on a Bruker Reflex III (Bruker, Breman, Germany) mass spectrometer operated in linear, positive ion mode with an N_2 laser. Laser power was used at the threshold required to produce a signal. The matrix used for each experiment was dithranol, and this was integrated into the analyte by dissolving a mixture of dithranol and the analyte in DMSO, THF, or CH_2Cl_2. Electron absorption spectroscopy data was obtained using a Varian Cary 5000 UV−vis−NIR spectrophotometer, in a cell with a 0.5 mm path length with an analyte concentration of approximately 1 mM. Infrared experiments were carried out on a Perkin-Elmer Spectrum Two FT-IR spectrometer using a solution cell with KBr plates. In each experiment the analyte was dissolved in either CH_2Cl_2, or a solvent mixture of DMSO (5% v/v) in CH_2Cl_2. Electrochemical studies were carried out in an N_2-purged solution containing the electrolyte NBu_4PF_6 (0.1 M) and sample (5 mM concentration). In each case, a standard three-electrode setup was implemented with a platinum disk working electrode, a platinum wire as a counter electrode, and a Ag/AgCl electrode as a pseudoreference. After each experiment, a small amount of ferrocene was added as an internal reference, and all data reported herein is reported versus the Fc/Fc^+ couple. All potentials are reported at a scan rate of 100 mV/s.

Materials. All experimental procedures were performed under an inert atmosphere of argon and using standard Schlenk-line and glovebox techniques. All solvents were obtained from a "Grubbs" solvent purification system with the exception of DMSO and 1,2-dichlorobenzene which were dried via vacuum distillation over CaH_2 and then degassed with argon. $Mo_2(OAc)_4$,[64] M_2TiPB_4 (M = Mo,[17] W[26]) and H_2DON[65] were synthesized according to previously published methods. H_2DON was ground to a fine powder prior to

dx.doi.org/10.1021/ic401555g | Inorg. Chem. 2013, 52, 9683−9691

each reaction. All other compounds were obtained from commercial sources and used without further purification.

Synthesis of $Mo_2(TiPB)_3HDON$, 1a. The synthesis of this compound has been previously reported,[45] but we include here a summary of the IR, UV−vis and ^1H NMR data in different solvents. ^1H NMR (400 MHz, CD_2Cl_2) δ 12.29 (s, 1 H, N-*H*), 7.78 (d, J_{HH} = 9.0 Hz, 1 H, aromatic HDON), 7.67 (d, J_{HH} = 9.0 Hz, 1 H, aromatic HDON), 7.27 (s, 2 H, aromatic TiPB), 7.11 (d, J_{HH} = 9.0 Hz, 1 H, aromatic HDON), 6.98 (s, 4 H, aromatic TiPB), 6.66 (d, J_{HH} = 9.0 Hz, 1 H, aromatic HDON), 3.66 (septet, J_{HH} = 7.0 Hz, 2 H, C*H*$(CH_3)_2$), 3.04, (septet, J_{HH} = 7.0 Hz, 1 H, C*H*$(CH_3)_2$), 2.83 (septet, J_{HH} = 7.0 Hz, 6 H, C*H*$(CH_3)_2$), 1.38 (d, J_{HH} = 7.0 Hz, 6 H, CH$(CH_3)_2$), 1.36 (d, J_{HH} = 7.0 Hz, 12 H, CH$(CH_3)_2$), 1.23 (d, J_{HH} = 7.0 Hz, 12 H, CH$(CH_3)_2$), 1.02 (d, J_{HH} = 7.0 Hz, 12 H, CH$(CH_3)_2$), 0.94 (d, J_{HH} = 7.0 Hz, 12 H, CH$(CH_3)_2$). ^1H NMR (400 MHz, $(CD_3)_2SO$) δ 10.34 (s, 1 H, N-*H*), 7.95 (d, J_{HH} = 9.0 Hz, 1 H, aromatic HDON), 7.91 (d, J_{HH} = 9.0 Hz, 1 H, aromatic HDON), 7.25 (s, 2 H, aromatic TiPB), 7.04 (s, 4 H, aromatic TiPB), 7.01 (d J_{HH} = 9.0 Hz, 1 H, aromatic HDON), 6.23 (d, J_{HH} = 9.0 Hz, 1 H, aromatic HDON), 3.70 (septet, J_{HH} = 7.0 Hz, 1 H, C*H*$(CH_3)_2$), 3.00 (septet, J_{HH} = 7.0 Hz, 1 H, C*H*$(CH_3)_2$), 2.85 (m, 7 H, C*H*$(CH_3)_2$), 1.13 (m, 53 H, CH$(CH_3)_2$). IR (CH_2Cl_2/DMSO (20:1 v/v)): ν_{max} cm^{-1}; 3108 (br, w), 3038 (w), 2966 (s), 2949 (m), 2874 (m), 2815 (w), 1617 (s), 1616 (s), 1591 (w), 1534 (sh, w), 1506 (s), 1509 (sh, m), 1465 (m), 1406 (s). UV−vis (DMSO); λ_{max} nm (ε, M^{-1} cm^{-1}) 321 (sh) (10074), 334 (12488), 350 (11865), 430 (4152).

Synthesis of $W_2(TiPB)_3HDON$, 1b. A Schlenk tube was charged with $W_2(TiPB)_4$ (0.148 g, 0.11 mmol) and 2,7-dihydroxy-1,8-naphthyridine (H_2DON) (0.016 g, 0.10 mmol). Dry toluene (30 mL) was added via cannula and the reaction was stirred for 48 h, whereupon a dark brown solution formed. The solvent was removed in vacuo, and the resulting solid washed with dry hexane (15 mL) to yield a dark green powder (0.118 g, 0.093 mmol, 93%). ^1H NMR (400 MHz, CD_2Cl_2) δ 12.67 (s, 1 H, N−H), 7.82 (m, 1 H, aromatic HDON), 7.27 (s, 2 H, aromatic TiPB), 7.17 (m, 2 H, aromatic HDON), 6.96 (s, 4 H, aromatic TiPB), 6.82 (m, 1 H, aromatic HDON), 3.60 (m, 2.5 H C*H*$(CH_3)_2$), 2.87, (m, 2.5 H, C*H*$(CH_3)_2$), 2.66 (septet, J_{HH} = 7.0 Hz, 4 H, C*H*$(CH_3)_2$), 1.34 (d, J_{HH} = 7.0 Hz, 13 H, CH$(CH_3)_2$), 1.22 (d, J_{HH} = 7.0 Hz, 15 H, CH$(CH_3)_2$), 0.98 (d, J_{HH} = 7.0 Hz, 13 H, CH$(CH_3)_2$), 0.92 (d, J_{HH} = 7.0 Hz, 13 H, CH$(CH_3)_2$). UV−vis (DMSO); λ_{max} nm (ε, M^{-1} cm^{-1}) 300 (sh) (7650), 331 (11000), 346 (8660), 442 (6900), 507 (6680), 573 (6370). MALDI-TOF-MS calcd. monoisotopic MW for $W_2C_{56}H_{74}N_2O_8$, 1270.45, found m/z 1270.40 (M^+). The compound is too air-sensitive to obtain accurate elemental analysis, which has been encountered in previous studies on related ditungsten compounds.[66]

Synthesis of $Mo_2(TiPB)_2(HDON)(O_2CCH_2Cl)$, 1c. $Mo_2(TiPB)_3HDON$ (0.109 g, 0.1 mmol) and finely ground monochloroacetic acid (0.009 g, 0.1 mmol) were placed in a flame-dried Schlenk tube. Toluene (20 mL) was added, and the reaction was stirred for 24 h to afford a light orange precipitate. The solution was concentrated to around 10% volume in vacuo, and hexane (15 mL) was added. The resulting precipitate was isolated via centrifugation, and dried in vacuo to obtain a light orange powder (0.080 g, 0.085 mmol. 85%). ^1H NMR (400 MHz, $(CD_3)SO$) δ 9.92 (s, 1 H, N-*H*), 7.94 (d, J_{HH} = 9.0 Hz, 1 H, aromatic HDON), 7.93 (d, J_{HH} = 9.0 Hz, 1 H, aromatic HDON), 7.08 (d, J_{HH} = 9.0 Hz, 1 H, aromatic HDON), 7.05 (s, 4 H, aromatic TiPB), 6.19 (dd, J_{HH} = 9.0 Hz, J_{HH} = 2 Hz, 1 H, aromatic HDON), 4.96 (s, 2 H, Cl*H*$_2$CCOO), 2.90 (septet, J_{HH} = 7.0 Hz, 3 H, C*H*$(CH_3)_2$), 2.85−2.72 (m, 3 H, C*H*$(CH_3)_2$) 1.21 (d, J_{HH} = 7.0 Hz, 24 H, CH$(CH_3)_2$), 1.15 (d, J_{HH} = 7.0 Hz, 12 H, CH$(CH_3)_2$). UV−vis (DMSO); λ_{max} nm (ε, M^{-1} cm^{-1}) 320 (sh) (29600), 331 (35100), 349 (30000), 421 (7190). MALDI-TOF-MS calcd. monoisotopic MW for $Mo_2C_{42}H_{53}N_2O_8Cl$, 944.2 found m/z 944.3. (M^+). Anal. Calcd for $Mo_2C_{42}H_{53}N_2O_8Cl$: C, 53.59; H, 5.68; N, 2.98; Cl, 3.77. Found: C, 53.04; H, 5.51; N, 3.28; Cl, 3.75%.

Synthesis of $Mo_2(TiPB)_2(HDON)_2$, 2. A Schlenk tube was charged with $Mo_2(TiPB)_4$ (0.1193 g, 0.1 mmol) and H_2DON (0.032 g, 0.2 mmol). Toluene (30 mL) was added via cannula, and the mixture stirred at 60 °C for 48 h. The resulting solution was concentrated to around one-third of the original volume in vacuo, and the product precipitated by addition of hexane (30 mL). The solid was isolated by centrifugation and dried in vacuo to yield the product as an orange powder (0.080 g, 0.08 mmol, 80%). ^1H NMR (400 MHz, $(CD_3)_2SO$) two regioisomers can be determined (*trans*-1,1 and *trans*-2,0), which exist in a 1.7: 1 ratio. *trans-1,1*: δ 10.23 (s, 2 H, N*H*), 8.00−7.85 (m, 2 H, aromatic HDON), 7.04 (s, 2 H, aromatic TiPB), 6.98 (d, J_{HH} = 9.0 Hz, 1 H, aromatic HDON), 2.94−2.57 (m, 6 H, C*H*$(CH_3)_2$), 1.23−0.72 (m, 36 H CH$(CH_3)_2$). *trans-2,0*: δ 10.16 (s, 2 H, N*H*), 8.00−7.85 (m, 2 H, aromatic HDON), 7.12 (d, J_{HH} = 9.0 Hz, 1 H, aromatic HDON), 7.04 (s, 2 H, aromatic TiPB), 2.94−2.57 (m, 6 H, C*H*$(CH_3)_2$), 1.23−0.72 (m, 36 H, CH$(CH_3)_2$). IR (CH_2Cl_2/DMSO (10:1 v/v)): ν_{max} cm^{-1}; 3110 (br, w), 3504 (w), 2968 (s), 2950 (m), 2876 (m), 2823 (w) 1715 (w), 1672 (s), 1617 (s), 1615 (s), 1534 (w), 1508 (s), 1466 (m), 1419 (s). UV−vis (DMSO); λ_{max} nm (ε, M^{-1} cm^{-1}) 332 (32874), 346 (sh) (23418), 448 (4398). MALDI-TOF-MS calcd. monoisotopic MW for $Mo_2C_{48}H_{56}O_8N_4$, 1012.2, found m/z 1012.8 (M^+). Anal. Calcd for $Mo_2C_{48}H_{56}O_8N_4$: C, 57.14; H, 5.59; N, 5.55. Found: C, 56.78; H, 5.88; N, 5.11.

Synthesis of Mo_2HDON_4, 3. $Mo_2(OAc)_4$ (0.200 g, 0.46 mmol) and H_2DON (0.313 g, 1.93 mmol) were placed in a Schlenk tube, and 1,2-dichlorobenzene (30 mL) was added. The reaction was heated to reflux and left for 18 h. Upon cooling to room temperature the product precipitated as a red-brown precipitate, which was isolated by filtration, washed with hexane (2 × 30 mL), and dried in vacuo (0.366g, 0.44 mmol, 95%). ^1H NMR (400 MHz, $(CD_3)_2SO$) δ 10.29, 10.16, 9.94 (three singlets, 4 H total, N*H*), 7.94−7.65 (m, 8 H, aromatic HDON), 7.10−6.90 (m, 4 H, aromatic HDON), 6.25−6.05 (m, 4 H aromatic HDON). UV−vis (DMSO); λ_{max} nm (ε, M^{-1} cm^{-1}) 321 (39850), 331 (39150), 346 (35550), 461 (9750). MALDI-TOF-MS calcd. monoisotopic MW for $Mo_2C_{32}H_{20}O_8N_8$, 840.00, found m/z 839.8 (M^+).

X-ray Crystallography. Data were collected and measured on a Bruker Smart CCD area detector with Oxford Cryosystems low temperature system. After integration of the raw data and merging of equivalent reflections, an empirical absorption correction was applied (SADABS) based on comparison of multiple symmetry-equivalent measurements.[67] The structures were solved by direct methods (SHELXS-97)[68] and refined by full-matrix least-squares on weighted F^2 values for all reflections.[69] All hydrogens were included in the models at calculated positions using a riding model with U(H) = 1.5 × U_{eq} (bonded carbon atom) for methyl and hydrogens and U(H) = 1.2 × U_{eq} (bonded carbon atom) for methine, methylene, and aromatic hydrogens.

For $2(DMSO)_2{\cdot}4DMSO$, one of the isopropyl groups on the TiPB ligand was disordered and modeled in two positions isotropically with 0.58/0.42 site occupancies. One dimethyl sulfoxide molecule (S3) was disordered over two positions (0.61/0.39 site occupancies); only the associated sulfur atoms were refined anisotropically. Another dimethyl sulfoxide molecule (S2) was disordered about two positions along the crystallographic C_2 axis and another about a center of inversion (S4); both molecules had equal disorder (0.5 occupancy) about both positions and the atoms refined isotropically. The disorder associated with the center of inversion for S4 resulted in one of the carbon atoms (C32) and an oxygen atom (O8) to be disordered over the same site, which was modeled using the EXYZ constraint and that each atom has 0.5 site occupancy. The residual electron density peak of 2.620 e $Å^{-3}$ is associated with the disorder observed in these solvate molecules.

The DMSO molecules in $3(DMSO)_2{\cdot}2DMSO$ were disordered over two positions, and were modeled with site occupancies of 0.59/0.41 (S1) and 0.54/0.44 (S2). Experimental data relating to the structure determination of both compounds is shown in Table 4. The supplementary crystallographic data for these compounds are contained in CCDC 945118 (**2**) and 945119 (**3**).

Theoretical Methods. Molecular structure calculations were performed using DFT as implemented in the Gaussian 09 software package.[70] The M06 functional[71] and the 6-311G(d,p) basis set[72−74] were used for H, C, O, and N, along with the SDD energy consistent pseudopotentials[75] for molybdenum and tungsten. The same functional/basis set combinations have been successfully employed in a

dx.doi.org/10.1021/ic401555g | Inorg. Chem. 2013, 52, 9683−9691

Table 4. Crystal Data for 2(DMSO)$_2$·4DMSO and 3(DMSO)$_2$·2DMSO

	2(DMSO)$_2$·4DMSO	3(DMSO)$_2$·2DMSO
empirical formula	$C_{60}H_{92}Mo_2N_4O_{14}S_6$	$C_{40}H_{44}Mo_2N_8O_{12}S_4$
formula weight	1477.62	1148.95
temperature (K)	150(2)	150(2)
wavelength (Å)	0.71073	0.71073
crystal system, space group	monoclinic, $C2/c$	monoclinic, $P2_1/n$
a (Å)	33.0716(7)	15.2138(11)
b (Å)	12.4762(3)	9.9307(7)
c (Å)	17.4131(4)	15.6547(11)
α (deg)	90	90
β (deg)	92.4240(10)	106.240(4)
γ (deg)	90	90
volume (Å^3)	7178.4(3)	2270.8(3)
Z, Calculated density (g cm^{-3})	4, 1.367	2, 1.680
F(000)	3088	1168
θ range for data collection (deg)	1.74−27.54	2.20−25.07
limiting indices	$-41 \le h \le 42$, $-16 \le k \le 16$, $-22 \le l \le 22$	$-17 \le h \le 18$, $-11 \le k \le 11$, $-18 \le l \le 17$
reflections collected/ unique	45689/8174 [R_{int} = 0.0515]	19305/4024 [R_{int} = 0.1632]
completeness	to θ = 27.54; 98.80%	to θ = 25.07; 99.90%
data/restraints/parameters	8174/24/372	4024/91/358
goodness-of-fit on F^2	1.058	0.956
final R indices [$I > 2\sigma(I)$]	R_1 = 0.0604, wR_2 = 0.1582	R_1 = 0.0629, wR_2 = 0.1148
R indices (all data)	R_1 = 0.0791, wR_2 = 0.1729	R_1 = 0.1659, wR_2 = 0.1507
largest diff. peak and hole (e Å^{-3})	2.620 and −1.242	0.394 and −0.464

study on related quadruply bonded compounds which have weak metal−ligand interactions.[76]

Geometry optimizations of the model compounds $Mo_2(O_2CH)_3(HDON)$ (**1a**′), $W_2(O_2CH)_3(HDON)$ (**1b**′), $Mo_2(O_2CH)_2(HDON)_2$ (**2**′), and $Mo_2(HDON)_4$ (**3**′) were performed without symmetry constraints. All optimizations were performed in a DMSO solvent cavity using the polarizable continuum model, as implemented in Gaussian 09, and the structures were confirmed to be minima on the potential energy surface using harmonic vibrational frequency analysis.

■ ASSOCIATED CONTENT

Ⓢ Supporting Information

^{1}H NMR spectra of [**1a**]$_2$ at different concentrations, IR spectra of **1a** and [**1a**]$_2$, cyclic voltammograms of **1a**, **1b**, and **1c**, and final calculated atomic coordinates for all compounds. This material is available free of charge via the Internet at http://pubs.acs.org.

■ AUTHOR INFORMATION

Corresponding Author

*E-mail: n.patmore@sheffield.ac.uk.

Notes

The authors declare no competing financial interest.

■ ACKNOWLEDGMENTS

The Royal Society is gratefully acknowledged for a University Research Fellowship (N.J.P.). Dr. Anthony Meijer and Mr. Harry Adams are thanked for computational assistance and crystallographic help. The University of Sheffield is thanked for a PhD studentship (L.A.W.).

■ REFERENCES

(1) Cotton, F. A.; Murillo, C. A.; Walton, R. A. *Multiple Bonds Between Metal Atoms*, 3rd ed.; Springer Science and Business Media, Inc: New York, 2005.

(2) *Special Issue: Metal-Organic Frameworks*; Zhou, H.-C.; Long, J. R.; Yaghi, O. M., Eds.; *Chem. Rev.*, **2012**; *112*, 673−1268.

(3) Dincă, M.; Long, J. R. *Angew. Chem., Int. Ed.* **2008**, *47*, 6766.

(4) Berry, J. F. *Dalton Trans.* **2012**, *41*, 700.

(5) Davies, H. M. L.; Manning, J. R. *Nature* **2008**, *451*, 417.

(6) Doyle, M. P.; Duffy, R.; Ratnikov, M.; Zhou, L. *Chem. Rev.* **2010**, *110*, 704.

(7) (a) Kumar, D. K.; Filatov, A. S.; Napier, M.; Sun, J.; Dikarev, E. V.; Petrukhina, M. A. *Inorg. Chem.* **2012**, *51*, 4855. (b) Villalobos, L.; Cao, Z.; Fanwick, P. E.; Ren, T. *Dalton Trans.* **2012**, *41*, 644.

(8) Fishman, R. S.; Satoshi, O.; Miller, J. S. *Phys. Rev. B* **2009**, *80*, 140416/1.

(9) Mikuriya, M.; Yoshioka, D.; Borta, A.; Luneau, D.; Matoga, D.; Szklarzewicz, J.; Handa, M. *New J. Chem.* **2011**, *35*, 1226.

(10) Motokawa, N.; Matsunaga, S.; Takaishi, S.; Miyasaka, H.; Yamashita, M.; Dunbar, K. R. *J. Am. Chem. Soc.* **2010**, *132*, 11943.

(11) Cummings, S. P.; Cao, Z.; Fanwick, P. E.; Kharlamova, A.; Ren, T. *Inorg. Chem.* **2012**, *51*, 7561.

(12) (a) Olea, D.; González-Prieto, R.; Priego, J. L.; Barral, M. C.; de Pablo, P. J.; Torres, M. R.; Gómez-Herrero, J.; Jiménez-Aparicio, R.; Zamora, F. *Chem. Commun.* **2007**, 1591. (b) Amo-Ochoa, P.; Jiménez-Aparicio, R.; Torres, M. R.; Urbanos, F. A.; Gallego, A.; Gómez-García, C. J. *Eur. J. Inorg. Chem.* **2010**, 4924.

(13) Berry, J. F.; Cotton, F. A.; Murillo, C. A. *Organometallics* **2004**, *23*, 2503.

(14) Ismayilov, R. H.; Wang, W.-Z.; Wang, R.-R.; Yeh, C.-Y.; Lee, G.-H.; Peng, S.-M. *Chem. Commun.* **2007**, 1121.

(15) Georgiev, V. P.; Mohan, P. J.; DeBrincat, D.; E., M. J. *Coord. Chem. Rev.* **2013**, *257*, 290.

(16) Blum, A. S.; Ren, T.; Parish, D. A.; Trammell, S. A.; Moore, M. H.; Kushmerick, J. G.; Xu, G.-L.; Deschamps, J. R.; Pollack, S. K.; Shashidhar, R. *J. Am. Chem. Soc.* **2005**, *127*, 10010.

(17) Cotton, F. A.; Daniels, L. M.; Hillard, E. A.; Murillo, C. A. *Inorg. Chem.* **2002**, *41*, 1639.

(18) Chisholm, M. H.; D'Acchioli, J. S.; Pate, B. D.; Patmore, N. J.; Dalal, N. S.; Zipse, D. J. *Inorg. Chem.* **2005**, *44*, 1061.

(19) Nippe, M.; Goodman, S. M.; Fry, C. G.; Berry, J. F. *J. Am. Chem. Soc.* **2011**, *133*, 2856.

(20) Hicks, J.; Ring, S. P.; Patmore, N. J. *Dalton Trans.* **2012**, *41*, 6641.

(21) Nippe, M.; Bill, E.; Berry, J. F. *Inorg. Chem.* **2011**, 7650.

(22) Nippe, M.; Turov, Y.; Berry, J. F. *Inorg. Chem.* **2011**, *50*, 10592.

(23) Dolinar, B. S.; Berry, J. F. *Inorg. Chem.* **2013**, *52*, 4658.

(24) Hopkins, M. D.; Gray, H. B. *J. Am. Chem. Soc.* **1984**, *106*, 2468.

(25) Alberding, B. G.; Chisholm, M. H.; Gustafson, T. L. *Inorg. Chem.* **2012**, *51*, 491.

(26) Alberding, B. G.; Chisholm, M. H.; Chou, Y.-H.; Gallucci, J. C.; Ghosh, Y.; Gustafson, T. L.; Patmore, N. J.; Reed, C. R.; Turro, C. *Inorg. Chem.* **2009**, *48*, 4394.

(27) Alberding, B. G.; Chisholm, M. H.; Ghosh, Y.; Gustafson, T. L.; Liu, Y.; Turro, C. *Inorg. Chem.* **2009**, *48*, 8536.

(28) Alberding, B. G.; Chisholm, M. H.; Chou, Y.-H.; Ghosh, Y.; Gustafson, T. L.; Liu, Y.; Turro, C. *Inorg. Chem.* **2009**, *48*, 11187.

(29) Alberding, B. G.; Chisholm, M. H.; Gallucci, J. C.; Ghosh, Y.; Gustafson, T. L. *Proc. Natl. Acad. Sci. U.S.A.* **2011**, *108*, 8152.

(30) Brown-Xu, S. E.; Chisholm, M. H.; Durr, C. B.; Spilker, T. F. *J. Am. Chem. Soc.* **2013**, *135*, 8254.

(31) Cotton, F. A.; Lin, C.; Murillo, C. A. *Acc. Chem. Res.* **2001**, *34*, 759.

(32) Cotton, F. A.; Lin, C.; Murillo, C. A. *Proc. Natl. Acad. Sci. U.S.A.* **2002**, *99*, 4810.

(33) Chisholm, M. H.; Macintosh, A. M. *Chem. Rev.* **2005**, *105*, 2949.

(34) Köberl, M.; Cokoja, M.; Herrmann, W. A.; Kühn, F. E. *Dalton Trans.* **2011**, *40*, 6834.
(35) Cotton, F. A.; Lin, C.; Murillo, C. A. *Inorg. Chem.* **2001**, *40*, 575.
(36) Chisholm, M. H.; Patmore, N. J.; Reed, C. R.; Singh, N. *Inorg. Chem.* **2010**, *49*, 7116.
(37) Cotton, F. A.; Daniels, L. M.; Lin, C.; Murillo, C. A. *J. Am. Chem. Soc.* **1999**, *121*, 4538.
(38) Köberl, M.; Cokoja, M.; Bechlars, B.; Herdtweck, E.; Kühn, F. E. *Dalton Trans.* **2011**, *40*, 11490.
(39) Li, J.-R.; Yakovenko, A. A.; Lu, W.; Timmons, D. J.; Zhuang, W.; Yuan, D.; Zhou, H.-C. *J. Am. Chem. Soc.* **2010**, *132*, 17599.
(40) Brammer, L. *Dalton Trans.* **2003**, 3145.
(41) Lynam, J. M. *Dalton Trans.* **2008**, 4067.
(42) Cowley, M. J.; Lynam, J. M.; Whitwood, A. C. *Dalton Trans.* **2007**, 4427.
(43) Pogozhev, D.; Baudron, S. A.; Hosseini, M. W. *Dalton Trans.* **2011**, *40*, 7403.
(44) Bera, J. K.; Vo, T.-T.; Walton, R. A.; Dunbar, K. R. *Polyhedron* **2003**, *22*, 3009.
(45) Wilkinson, L. A.; McNeill, L.; Meijer, A. J. H. M.; Patmore, N. J. *J. Am. Chem. Soc.* **2013**, *135*, 1723.
(46) Goeltz, J. C.; Kubiak, C. P. *J. Am. Chem. Soc.* **2010**, *132*, 17390.
(47) Chisholm, M. H.; Patmore, N. J. *Acc. Chem. Res.* **2007**, *40*, 19.
(48) Cayton, R. H.; Chisholm, M. H.; Huffman, J. C.; Lobkovsky, E. B. *J. Am. Chem. Soc.* **1991**, *113*, 8709.
(49) Alberding, B. G.; Chisholm, M. H.; Lear, B. J.; Naseri, V.; Reed, C. R. *Dalton Trans.* **2011**, *40*, 10658.
(50) Forlani, L.; Cristoni, G.; Boga, C.; Todesco, P. E.; Vecchio, E. D.; Monari, M. *ARKIVOC* **2002**, *11*, 198.
(51) Kadish, K. M.; Wang, L.-L.; Thuriere, A.; Van Caemelbecke, E.; Bear, J. L. *Inorg. Chem.* **2003**, *42*, 834.
(52) Dequeant, M. Q.; Ren, T. *J. Cluster Sci.* **2006**, *17*, 479.
(53) Majumdar, M.; Patra, S. K.; Kannan, M.; Dunbar, K. R.; Bera, J. K. *Inorg. Chem.* **2008**, *47*, 2212.
(54) Yang, M.; Szyc, L.; Dreyer, J.; Nibbering, E. T. J.; Elsaesser, T. *J. Phys. Chem. A* **2010**, *114*, 12195.
(55) Matsuda, Y.; Ebata, T.; Mikami, N. *J. Chem. Phys.* **1999**, *110*, 8397.
(56) Richardson, D. E.; Taube, H. *Inorg. Chem.* **1981**, *20*, 1278.
(57) D'Alessandro, D. M.; Keene, F. R. *Dalton Trans.* **2004**, 3950.
(58) Barriere, F.; Camire, N.; Geiger, W. E.; Mueller-Westerhoff, U. T.; Sanders, R. *J. Am. Chem. Soc.* **2002**, *124*, 7262.
(59) Chisholm, M. H.; Clark, R. J. H.; Gallucci, J.; Hadad, C. M.; Patmore, N. J. *J. Am. Chem. Soc.* **2004**, *126*, 8303.
(60) Chisholm, M. H. *Proc. Natl. Acad. Sci. U.S.A.* **2007**, *104*, 2563.
(61) Chisholm, M. H.; Feil, F.; Hadad, C. M.; Patmore, N. J. *J. Am. Chem. Soc.* **2005**, *127*, 18150.
(62) Mayer, J. M. *Annu. Rev. Phys. Chem.* **2004**, *55*, 363.
(63) Huynh, M. H. V.; Meyer, T. J. *Chem. Rev.* **2007**, *107*, 5004.
(64) Brignole, A. B.; Cotton, F. A. *Inorg. Synth.* **1972**, *13*, 81.
(65) Newkome, G. R.; Garbis, S. J.; Majestic, V. K.; Fronczek, F. R.; Chiari, G. *J. Org. Chem.* **1981**, *46*, 833.
(66) Byrnes, M. J.; Chisholm, M. H.; Clark, R. J. H.; Gallucci, J. C.; Hadad, C. M.; Patmore, N. J. *Inorg. Chem.* **2004**, *43*, 6334.
(67) Sheldrick, G. M. *A Program for Absorption Correction with the Siemens SMART System*; University of Göttingen: Göttingen, Germany, 1996.
(68) Sheldrick, G. M. *Acta Crystallogr., Sect. A* **1990**, *46*, 467.
(69) *SHELXTL program system*, version 5.1; Bruker Analytical X-ray Instruments Inc.: Madison, WI, 1998.
(70) Frisch, M. J.; Trucks, G. W.; Schlegel, H. B.; Scuseria, G. E.; Robb, M. A.; Cheeseman, J. R.; Scalmani, G.; Barone, V.; Mennucci, B.; Petersson, G. A.; Nakatsuji, H.; Caricato, M.; Li, X.; Hratchian, H. P.; Izmaylov, A. F.; Bloino, J.; Zheng, G.; Sonnenberg, J. L.; Hada, M.; Ehara, M.; Toyota, K.; Fukuda, R.; Hasegawa, J.; Ishida, M.; Nakajima, T.; Honda, Y.; Kitao, O.; Nakai, H.; Vreven, T.; Montgomery, Jr., J. A.; Peralta, J. E.; Ogliaro, F.; Bearpark, M.; Heyd, J. J.; Brothers, E.; Kudin, K. N.; Staroverov, V. N.; Kobayashi, R.; Normand, J.; Raghavachari, K.; Rendell, A.; Burant, J. C.; Iyengar, S. S.; Tomasi, J.; Cossi, M.; Rega, N.; Millam, J. M.; Klene, M.; Knox, J. E.; Cross, J. B.; Bakken, V.; Adamo, C.; Jaramillo, J.; Gomperts, R.; Stratmann, R. E.; Yazyev, O.; Austin, A. J.; Cammi, R.; Pomelli, C.; Ochterski, J. W.; Martin, R. L.; Morokuma, K.; Zakrzewski, V. G.; Voth, G. A.; Salvador, P.; Dannenberg, J. J.; Dapprich, S.; Daniels, A. D.; Farkas, Ö.; Foresman, J. B.; Ortiz, J. V.; Cioslowski, J.; Fox, D. J. *Gaussian 09*, Revision C.01; Gaussian, Inc.: Wallingford, CT, 2009.
(71) Zhao, Y.; Truhlar, D. G. *Theor. Chem. Acc.* **2008**, *120*, 215.
(72) McLean, A. D.; Chandler, G. S. *J. Chem. Phys.* **1980**, *72*, 5639.
(73) Wachters, J. H. *J. Chem. Phys.* **1970**, *52*, 1033.
(74) Hay, P. J. *J. Chem. Phys.* **1977**, *66*, 4377.
(75) Andrae, D.; Haeussermann, U.; Dolg, M.; Preuss, H. *Theor. Chim. Acta* **1990**, *77*, 123.
(76) Carrasco, M.; Faust, M.; Peloso, R.; Rodríguez, A.; López-Serrano, J.; Alvarez, E.; Maya, C.; Power, P. P.; Carmona, E. *Chem. Commun.* **2012**, *48*, 3954.